OPTIMIZATION OF PMSG VARIABLE SPEED WIND ENERGY CONVERSION SYSTEM CONTROLLER PARAMETERS BY BIOGEOGRAPHY-BASED OPTIMIZATION

H. M. YASSIN eng.haitham.2007@gmail.com
H. H. HANAFY hanafy_hassan@hotmail.com
Mohab M. HALLOUDA hallouda@yahoo.com
Electrical Power & Machines Department, Faculty of Engineering, Cairo University, Giza 12613, Egypt,

***Abstract**: This paper presents an optimization procedure of maximum power point tracking method for direct-drive permanent-magnet synchronous generator (PMSG) wind generation system. The Field oriented control is used to control the frequency converter using the PI controllers to achieve maximum power point tracking. The setting of the parameters of the PI controllers used in the frequency converters is very difficult. . An optimization design procedure for frequency converter using Biogeography-based optimization (BBO) technique is presented in this paper.*

The constrained optimization problem is solved using Biogeography-based optimization and Genetic Algorithm. MATLAB-SIMULINK is used to evaluate the effectiveness of the proposed BBO technique. In order to verify the validity and the performance of the proposed controllers, the simulation results for a VSWT-PMSG using a PI controllers optimized by the BBO technique is compared with that obtained using Genetic Algorithm.

***Keywords:** Biogeography-based optimization, Variable speed wind turbine, MPPT, Field oriented control, Permanent magnet synchronous generators.*

Nomenclature

A	The blade swept area (m^2)
C_p	The power conversion coefficient
Es	The maximum phase voltage of the grid voltage
i_{ds} , i_{qs}	The d- and q-axes stator currents of PMSG
i_d , i_q	The d- and q-axes components of the output currents of the grid side converter
J	The total moment of inertia of the system
L_{ds} , L_{qs}	The d- and q-axes inductances of PMSG
L_d , L_q	The d- and q-axes components of the inductance of the filter
L_{gf}	The inductance of the filter between the grid side converter and the grid
P_g	The active power output of PMSG
P_W	The extracted mechanical power from the wind
Q_s	The reactive power output to the grid
R	The radius of the blade
R_s	The stator resistance of PMSG
R_{gf}	The resistance of the filter between the grid side converter and the grid.
T_e	The electromagnetic torque of PMSG
T_m	The mechanical torque of the turbine
V	The wind speed (m/s)
v_{ds} , v_{qs}	The d- and q-axes stator voltages of PMSG
v_d , v_q	The d- and q-axes components of the output voltages of the grid side converter
V_{dc}	The DC link voltage
ρ	The air density (Kg/m^3)
β	The blade pitch angle (deg.)
λ	The tip-speed ratio
ψ_f	The rotor magnetic flux of permanent magnet
ω_r	The electrical angular speed
ω_m	The rotational speed
Ω	The angular frequency of the grid voltage
θ_m	The electrical angular position of the rotor
θ_q	The angular position of the grid voltage

1. Introduction

Recently, with the rising demand of electricity, wind energy conversion system (WECS) has been attractive and competitive with conventional fossil fuel energy resources that it is safe, pollution free, inexhaustible and free in term of its natural existence. WECS has become one of the most important renewable sources of alternative energy for the future [1-2]. More than 35 GW of new wind power capacity was installed in 2013. The new global total at the end of 2013 was 318 GW, representing cumulative market growth of more than 12.3 %. By the year 2018, the global wind power capacity is expected to be 600 GW. In Egypt, 550 MW of wind power were installed. The total wind power installation is expected to be 7200 MW by 2020 [3].

There are two types of wind turbine systems which are fixed and variable speed wind turbines. Variable speed wind turbine (VSWT) is most commonly used with the wind power systems in

order to maximize energy captured at various wind speed. The variable-speed wind turbine systems have a wide speed range of operation and provide 10%-15% higher energy capture from the fixed speed types [4] and reduce the load on the drive-train and tower structure [5]. The wind power generators connected to the main power grid are generally of two types: double fed asynchronous and direct-drive permanent magnet synchronous generators. The high efficiency, power density, wide speed range, reliability and full isolation of the PMSG generator from the power grid make it preferred in variable speed wind systems [6–8]. The control method to capture the maximum power from wind turbines in the variable speed region is called a maximum power point tracking (MPPT) control. There are four categories of the MPPT methods in the wind turbine system; power signal feedback control, perturbation and observation control, tip-speed ratio control and optimal torque control [9-10].

Due to the decoupling of the generator system from the grid, the grid support and fault ride through can be achieved easily [11, 12]. So PMSG wind turbine is becoming more favored by the wind power industry.

The conventional PI controllers are very sensitive to parameter variations and the nonlinearity of dynamic systems. The setting of the parameters of the PI controllers used in the frequency converters of VSWT-PMSG generation system is exhausted. In [13], Genetic algorithm (GA) and response surface methodology (RSM) are used to optimally design the controller used in the frequency converter of a VSWT-PMSG. Generalized reduced gradient (GRG) algorithm is compared with the proposed Gas-RSM algorithm to verify the effectiveness of the designed parameters using GAs-RSM. An extremum-seeking (ES) optimization algorithm is performed to extract maximum power from a WECS in [14].

Modeling of natural process that used to solve problems of general optimization is first used to present the application of biogeography for optimization [15]. The biogeography-based optimization algorithm is similar to other evolutionary algorithms optimization techniques such as genetic algorithms (GAs), particle swarm optimization (PSO). The fourteen benchmarks optimization problems are used to compare BBO algorithm with other evolutionary algorithms optimization techniques to show significant advantages of the BBO algorithm [15].

In this paper, The Field oriented control is used to control the frequency converter using the PI controllers to achieve MPPT of VSWT-PMSG. The setting of the parameters of the PI controllers, using trial and error method which is commonly used for tuning PI controllers, used in the frequency converters of VSWT-PMSG generation system is time consumed and the desired accuracy is satisfied only within a short interval close to the desired operating point. So the objective of this paper is to optimize the parameters of PI controllers of the machine and grid side converters using BBO, and compare the results of this optimization technique with the results obtained using GA optimization technique.

The machine side converter (MSC) and grid side converter (GSC) controller parameters are determined by BBO and GA to optimize the performance indices. The minimization of the settling time, maximum overshoot and undershoot of the generator speed and the DC link voltage to track the reference values are considered as the performance indices to achieve MPPT.

In order to verify the validity and the performance of the proposed controllers using BBO, the simulation results for a VSWT-PMSG using a PI controllers optimized by the BBO based optimization technique is compared with that obtained using GA. The paper is divided as follows: in Section II, the modeling of the wind turbine, generator and the MPPT are described briefly. In Section III, control of the frequency converter used in VSWT-PMSG is presented. Section IV deals with the Biogeography-based optimization (BBO) technique. In Section V, the proposed optimization procedure is presented. Section VI presents the simulation results and discussion. Finally, some conclusion remarks are given in section VII.

2. Direct Drive PMSG Wind Turbine System

The direct-drive PMSG wind generation system is shown in Fig. 1, where the wind turbine is connected to the PMSG directly.

The electrical power generated by the PMSG is transmitted to a power grid via a variable-frequency converter, which consists of a machine-side converter and a grid-side converter connected back-to-back via a DC link.

2.1 Modeling of Wind Turbine

The extracted mechanical power from the wind is given by:

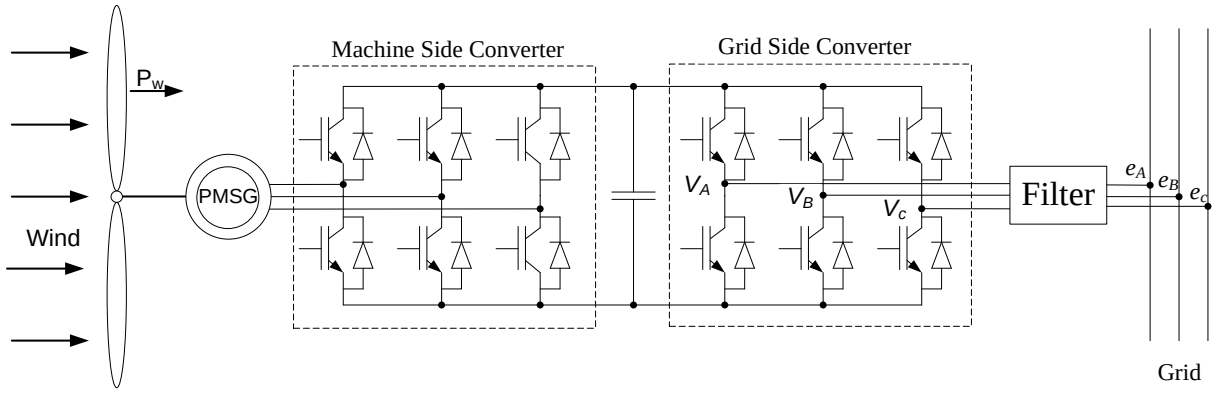

Fig. 1: Direct-drive PMSG wind power generation system.

$$P_W = \frac{1}{2}\rho A C_p(\lambda,\beta)V^3 \quad (1)$$

The power conversion coefficient is a function of the tip-speed ratio (TSR) and the blade pitch angle β (deg.), in which the TSR is defined as [16]:

$$\lambda = \frac{\omega_m R}{V} \quad (2)$$

Cp for given values of λ and β for both fixed and variable speed wind turbines is calculated based on the turbine characteristics in [17] by:

$$C_p(\lambda,\beta) = C_1\left(\frac{C_2}{\lambda_i} - C_3\beta - C_4\right)e^{\frac{-C_5}{\lambda_i}} + C_6\lambda \quad (3)$$

With

$$\frac{1}{\lambda_i} = \frac{1}{\lambda+0.08\beta} - \frac{0.035}{\beta^3+1} \quad (4)$$

The constants (C_1-C_6) are given in Appendix A. The power conversion coefficient versus tip speed ratio ($Cp - \lambda$) characteristics for different values of the pitch angle β is illustrated in Fig. 2. The maximum value of *Cp* (*Cp_max*) is achieved for $\beta = 0°$ and λ_{opt}. The maximum turbine power is found at a point of λopt and *Cp_max*. Fig. 3 depicts the turbine output power as a function of the rotor speed (P_w–ω_m) for different wind speeds with the blade pitch angle $\beta = 0°$. The dotted line show the locus of the maximum power point of the turbine which is used to determine the reference of active power.

2.2 Modeling of PMSG

The voltage equations of PMSG are given in d-q reference frame as [18-20]:

$$v_{ds} = R_s i_{ds} + L_{ds}\frac{di_{ds}}{dt} - \omega_r L_{qs} i_{qs} \quad (5)$$

$$v_{qs} = R_s i_{qs} + L_{qs}\frac{di_{qs}}{dt} + \omega_r L_{ds} i_{ds} + \omega_r \psi_f \quad (6)$$

Then, the electromagnetic torque Te is expressed as

$$T_e = p\{\psi_f i_{qs} + (L_{ds} - L_{qs})i_{ds} i_{qs}\} \quad (7)$$

The equation which lies at the base of the PMSG model is the mechanical equation given as

$$T_m - T_e = J\frac{d\omega_m}{dt} \quad (8)$$

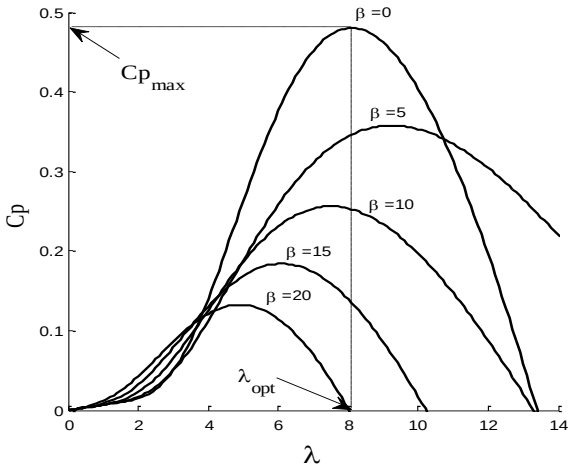

Fig. 2: power conversion coefficient versus tip speed ratio ($C_p - \lambda$) curve for different pitch angle

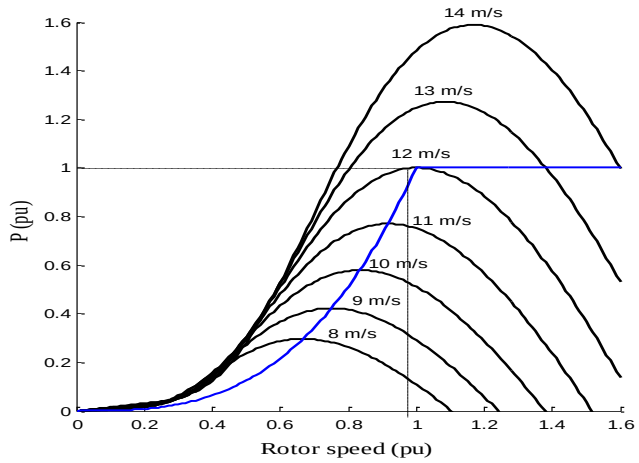

Fig. 3: Wind Turbine power characteristic (P_w–ω_m) curve with maximum power point tracking.

2.3 Grid Model

The input is a three phase voltage supply as follows:

$$e_A = E_s cos\omega t$$

$$e_B = E_s \cos\left(\omega t - \frac{2\pi}{3}\right) \quad (9)$$

$$e_C = E_s \cos\left(\omega t + \frac{2\pi}{3}\right)$$

The equation in the stationary A − B − C frame is

$$e_A = V_A - R_{gf} i_A - L_{gf} \frac{di_A}{dt}$$

$$e_B = V_B - R_{gf} i_B - L_{gf} \frac{di_B}{dt} \quad (10)$$

$$e_C = V_C - R_{gf} i_C - L_{gf} \frac{di_C}{dt}$$

Where i_A, i_B and i_C are the output currents and V_A, V_B and V_C are the output voltages of the grid side converter. The transformation of three phase stationary (ABC) to two phase stationary (α-β) is given by

$$e_\alpha = V_\alpha - R_{gf} i_\alpha - L_d \frac{di_\alpha}{dt} \quad (11)$$

$$e_\beta = V_\beta - R_{gf} i_\beta - L_q \frac{di_\beta}{dt} \quad (12)$$

Transformation from the stationary (α−β) to the synchronous (d−q) frame, which is rotating with the angular frequency ω, can be obtained as

$$v_d = R_{gf} i_d + L_d \frac{di_d}{dt} - \omega L_q i_q + e_d \quad (13)$$

$$v_q = R_{gf} i_q + L_q \frac{di_q}{dt} + \omega L_d i_d + e_q \quad (14)$$

For the angular position of the grid voltage (θ_g) which starts rotating with phase a as shown in Fig. 4, the amplitude of the phase voltages of the grid (e_A, e_B, e_C) which equals Es will be placed on the d- axis ($e_d = E_s$). The q-axis component voltage will be zero ($e_q = 0$). The output voltages of the grid side converter in the synchronous d − q frame are given by

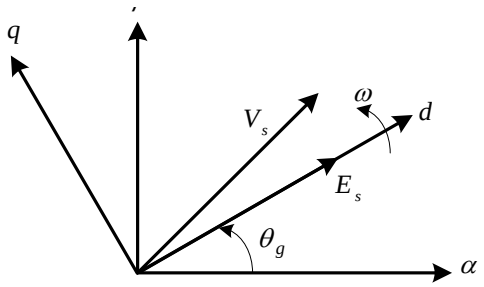

Fig. 4: Space vector diagram of the grid three phase voltages.

$$v_d = R_{gf} i_d + L_d \frac{di_d}{dt} - \omega L_q i_q + E_s \quad (15)$$

$$v_q = R_{gf} i_q + L_q \frac{di_q}{dt} + \omega L_d i_d \quad (16)$$

3. Control of PMSG Wind Turbine

3.1 Machine Side Converter Control

The objective of MSC control is to control the rotational speed of the PMSG to achieve variable-speed operation with the MPPT control. Field oriented control (FOC) is used in the control methodology as shown in Fig. 5. This type of control gives high performance. The control strategy requires three controllers, two for the currents in the inner loop and one for the rotor speed in the outer loop. The torque and flux can be controlled separately by the q and d-axis components of the generator current, respectively. Maximum Torque per Ampere control strategy is used to control the d and q-axis currents.

The d-axis component is set to zero, to minimize the stator current for a given torque, to produce maximum torque per ampere, therefore minimize the resistive losses [21].

In Fig. 5, the d and q reference voltages V_{ds}^* and V_{qs}^* are given by

$$V_{ds}^* = V_{ds}' + Compensation\ 1 \quad (17)$$

$$V_{qs}^* = V_{qs}' + Compensation\ 2 \quad (18)$$

These compensation terms are added to improve the transient response [21]. They are obtained from Equations (5) and (6).

$$Compensation\ 1 = -\omega_r L_{qs} i_{qs} \quad (19)$$

$$Compensation\ 2 = \omega_r L_{ds} i_{ds} + \omega_r \psi_f \quad (20)$$

Space Vector Pulse Width Modulation (SVPWM) is the technique used to create the duty cycles of the desired reference voltages.

3.2 Grid Side Converter Control

The main objective of this controller is to regulate the DC bus voltage (V_{dc}) and control the reactive power delivered to the grid. Fig. 6 shows the complete scheme of the FOC algorithm applied to the grid side converter. The control strategy requires four controllers, two for the currents in the inner loop, two for the DC bus voltage and the reactive power in the outer loop. The d-axis component of the grid current is controlled to maintain V_{dc} constant at a value that grantee the grid line to line voltage. The reactive power control is obtained through the q-axis

component of the grid current. The aim of the GSC control is to transfer all the active power produced by the wind turbine to the grid and also to produce no reactive power so that unity power factor is obtained.

Grid-voltage phase-locked loop (PLL) is employed to obtain the angular position of the grid voltage (θ_g) which is used to synchronize the output voltage of GSC with the grid voltage.

In Fig. 6, the d and q reference voltages V_d^* and V_q^* are given by

$$V_d^* = V_d' + Compensation\ 3 \quad (21)$$

$$V_q^* = V_q' + Compensation\ 4 \quad (22)$$

These compensation terms are added to improve the transient response [22]. They are given by

$$Compensation\ 3 = -\omega L_q i_q + E_s \quad (23)$$

$$Compensation\ 4 = \omega L_d i_d \quad (24)$$

4. Biogeography Based Optimization

At the beginning of the 19th century, Wallace [23] and Darwin [24] studied the biogeography. BBO is an evolutionary algorithm which simulates the biogeography of nearby islands. It is based on the mathematical study of the geographical distribution of biological organisms. The number of species which are able to live in the island is called habitat suitability index (HSI). Islands can share information with each other's by emigration and immigration of different species.

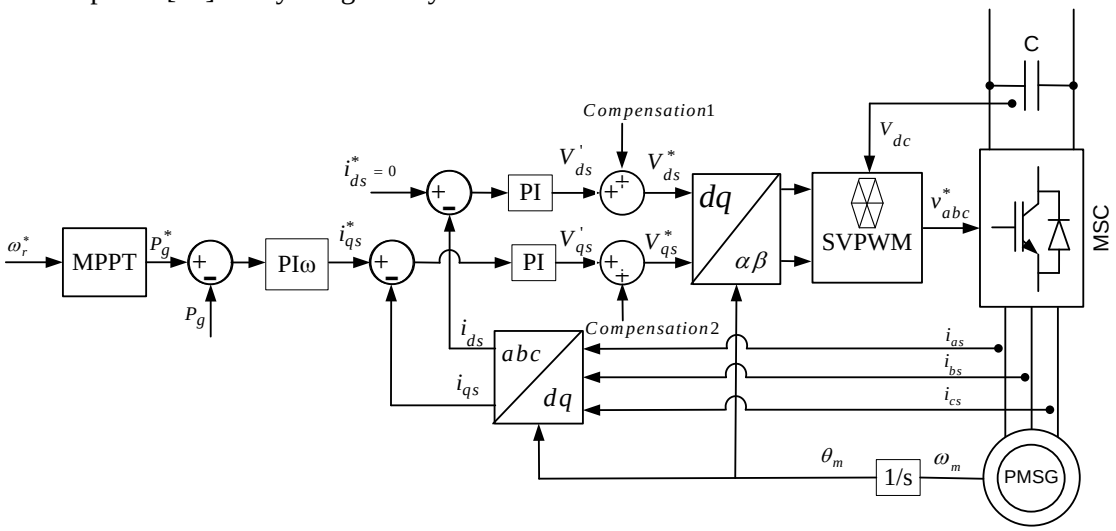

Fig. 5: Machine Side Converter Control

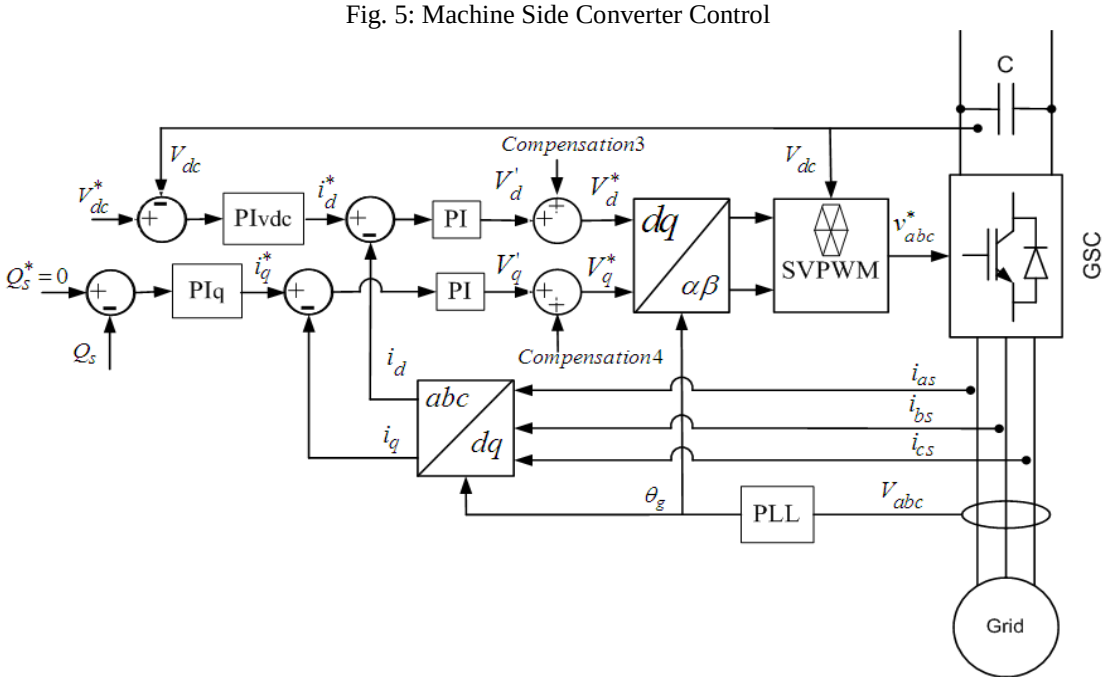

Fig. 6: Grid Side Converter Control

Extinction and migration of new species from one island to another is clearly described using mathematical models of biogeography.

The BBO's environment can be modeled as a group of islands where each island represents every possible solution to the optimization problem. Habitat suitability index (HSI) [25], which has a high similarity with the fitness of evolutionary algorithms (EAs) is high in those geographical areas which are suited as residences for biological species.

Habitability can be characterized by some variables which are called suitability index variables (SIVs).The problem dimension is obtained using the number of SIVs in each solution H.

An island with high HSI is corresponding to a good solution H of optimization problem while low HSI represents a poor one.

Islands that have a large number of species is said to have high HSI, while those islands that have a low number of species is said to have a low HSI.

Islands with a high HSI have many species that emigrate to nearby islands, simply by virtue of the large number of species that they host. Islands with a high HIS have low species immigration rate because they are already nearly saturated with species.

Therefore high HSI Islands are more static in their species distribution than low HSI Islands. By the same token, high HSI Islands have a high emigration rate; the large number of species on high HSI islands has many opportunities to emigrate to neighboring habitats. Habitats with a low HIS have high species immigration rate because of their sparse populations. This immigration of new species to low HSI habitats may raise the HSI of the habitat, because the suitability of a habitat is proportional to its biological diversity. However, if a habitat's HSI remains low, then the species that reside there will tend to go extinct, which will further open the way for additional immigration. Because of this low HSI habitats are more dynamic in their species distribution than high HSI habitats.

Improving the population is the way to solve problems in heuristic algorithms. The BBO migration strategy is similar to the global recombination approach of evolutionary strategies (ES) [26] in which many parents can contribute to a single offspring, but it differs in at least one important aspect. In ES global recombination is used to create new solutions, while in BBO migration is used to change existing solutions. Mutation is performed for the whole population in a manner similar to mutation in GAs (genetic algorithms).

5. Optimization Procedure

The optimal design of the converter's controllers of WECS is preferred to ensure the proper operation of the wind generation system under a wide range of wind speeds. Hence it is necessary to tune the parameters of the machine-side and grid-side converters.

As the MPPT of VSWT-PMSG is emphasized, the design variables are the proportional and integral gains of the generator speed controller (Kp_w, Ki_w) of the MSC, DC link voltage controller (Kp_v, Ki_v) and reactive power controller (Kp_q, Ki_q) of the GSC.
This section introduces the design procedure for coordinated tuning of MSC and GSC controllers using BBO optimization techniques.

This optimization requires a predefined of different parameter of BBO such as migration rates, mutation, and specifying of mutation rate, population size and number of generations, the details of the BBO design optimization method can be informally described as follows [15]:

1. Map the problem solutions to SIVs and habitats. Then, the BBO parameters can be initialized by initializing the maximum species count S_{max}, the maximum mutation rate m_{max}, the maximum migration rates E and I, and an elitism parameter.
2. Initialize a random set of islands, each island corresponding to a potential solution to the given problem.
3. For each island, map the HSI to the number of species, the immigration rate, and the emigration rate.
4. Modify each non-elite island by using immigration and emigration, then recompute each HSI.
5. The probability of each island's species count is updated. Then, according to its probability, mutate each non-elite island, and recompute each HSI.
6. Go to step (3) for the next iteration. This loop can be terminated after reaching an accepted solution or after a predefined number of generations.

Finally, the BBO Technique can be summarized by the Flow chart shown in Fig. 7.

6. Simulation Results

In this section, simulation studies are carried out via MATLAB/SIMULINK for 1.5-MW direct-drive PMSG wind turbine. The PMSG parameters used in the simulation are given in the Appendix B.
To determine the performance of optimum controller parameters, the system is tested with the wind speed changes in steps. The applied wind speed was

increased from 10 m/s to 12 m/s at 20 seconds and then it was decreased to 8 m/s at time = 40 second. These sudden changes in wind speeds are selected to perform the effectiveness of the proposed optimized controllers. The results of simulations are obtained for reactive power Q = 0 and DC link voltage Vdc = 1500 V to grantee the grid line to line voltage.

In order to verify the validity and effectiveness of the proposed controllers, the simulation results for a VSWT-PMSG using a PI controllers optimized by the BBO based optimization technique is compared to GA- optimized controllers. The comparison between BBO and GA is done for the same total population size, number of generations, mutation probability and fitness function tolerance. Table 1 shows the BBO and GA characteristics.

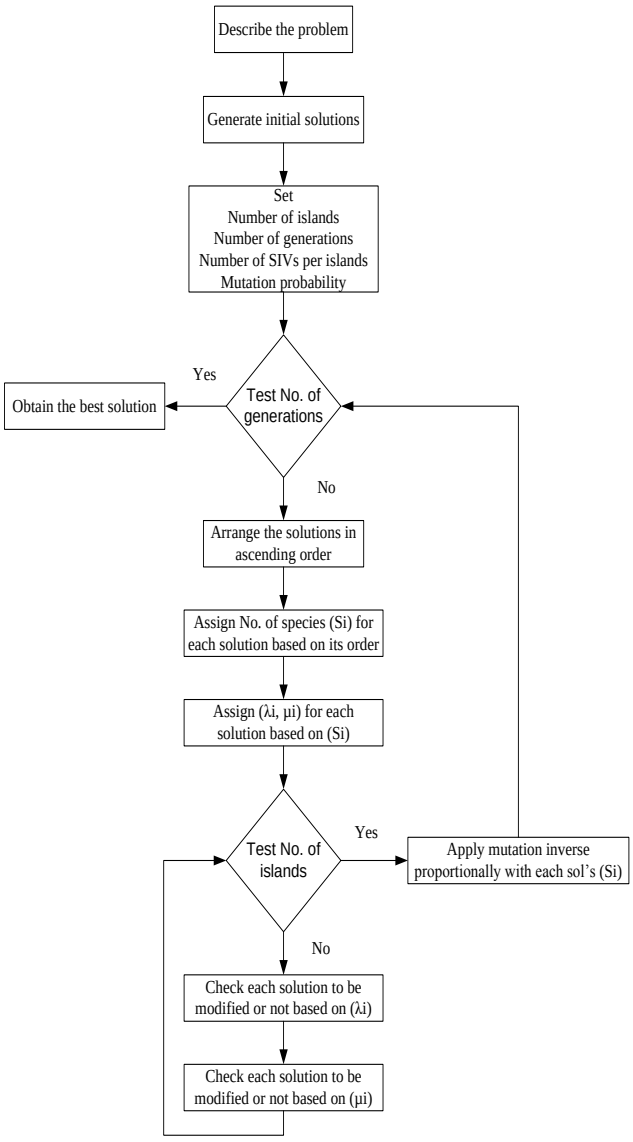

Fig. 7: BBO Technique flow chart sequence

Table1 BBO and GA Characteristics

Total population size	50
Number of generations	20
Mutation probability	0.005
Fitness function tolerance	1e-6

The parameters of the MSC and GSC controllers obtained using BBO and GA optimization techniques are given in Table 2. The proportional and integral gains of the current controllers of the MSC and GSC have the same values for the BBO and GA technique. The maximum power point tracking, the difference between the reference and actual generator speed, and the difference between the dc link reference voltage and actual voltage were considered as the objective functions. Maximum overshoot ($MPOS_{\omega r}$), maximum peak undershoot ($MPUS_{\omega r}$), settling time ($Tss_{\omega r}$) of the generator speed and the maximum peak overshoot ($MPOS_{Vdc}$), maximum peak undershoot ($MPUS_{Vdc}$) and settling time (Tss_{Vdc}) of DC link voltage are considered as constraints.

Fig. 8 shows the response of generator rotor speed with controller parameters optimized using BBO and GA for step change in wind speed, respectively. It can be seen from Fig. 9 that the generator speed response with BBO optimized controller parameters has a smaller overshoot of 3.3 % when compared to GA optimized controller parameters which has an overshoot of 6 %. The generator speed response also settles faster with BBO optimized controller parameters (4.1 s) than with GA optimized parameters (5.7 s).

Table 2 Optimal Values of Controller Parameters

Parameters	Tuned using BBO	Tuned using GA
Kpw	9.63	8.7
Kiw	7.19	7.6
Kpv	9.52	9.13
Kiv	7.81	6.89
Kpq	1.63	1.61
Kiq	9.75	9.43

Fig. 9 and Fig. 10 show the response of DC link voltage with controller parameters optimized using BBO and GA for step change in wind speed, respectively. It can be seen that The DC link voltage response also settles faster with BBO optimized controller parameters (4.28 s) than with GA optimized parameters (5.02 s). It can be noted from these figures that the DC link voltage response with BBO optimized controller parameters has a maximum overshoot of 2.73 % when compared to GA optimized controller parameters which has an

overshoot of 2.4 %. The controller performance indices with BBO and GA optimized parameters for step increase in wind speed are shown in Table 3.

The less maximum overshoot and settling time responses of the generator speed and DC link voltage for BBO optimization technique improve the low voltage ride through capability of PMSG wind generation system.

Table3 Performance Indices for Step Change in Wind Speed

Performance indices	For BBO	For GA
MPOSωr (%)	3.3	6
MPUSωr (%)	6.56	14.2
Tssωr (s)	4.1	5.7
MPOSVdc (%)	2.73	2.4
MPUSVdc (%)	1.53	1.8
TssVdc (s)	4.28	5.02

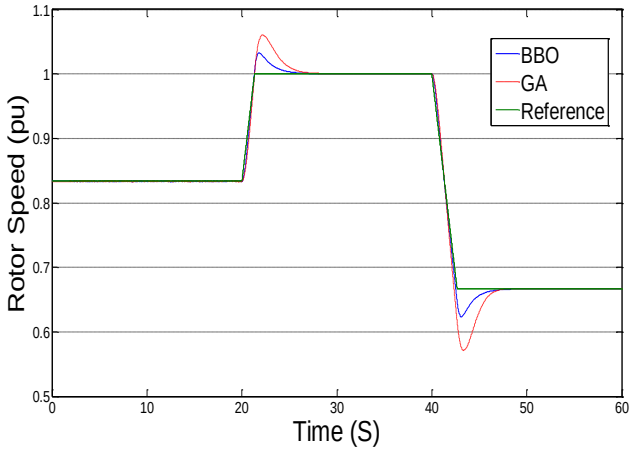

Fig. 8: Response of the rotor speed of PMSG

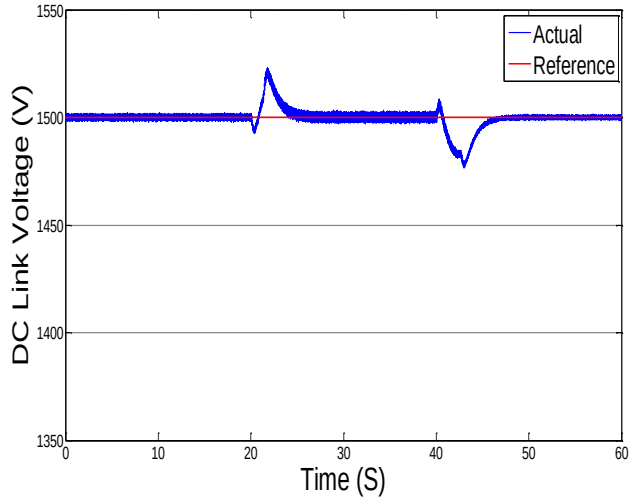

Fig. 9: Response of the DC link voltage for BBO technique.

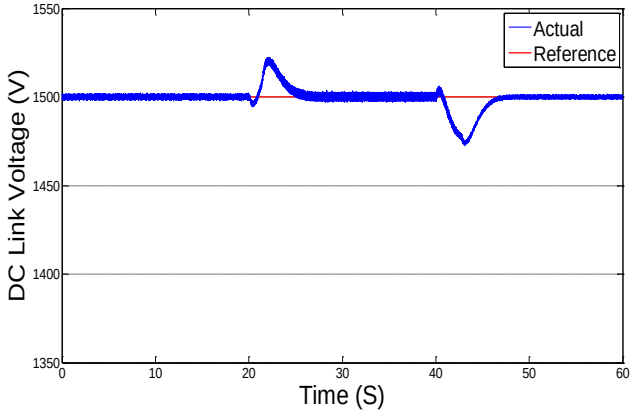

Fig. 10: Response of the DC link voltage for GA technique.

The active power responses of the turbine and generator for the BBO and GA optimization techniques are shown in Fig. 11 and Fig. 12, respectively. In Fig, 11 and 12, it can be noted that the generator active power tracks the maximum extracted mechanical power from the turbine to achieve MPPT at the corresponding wind speeds. At the time instant when wind speed steps up, the electrical torque is first reduced for faster speed regulation. As a result, the output active power drops at the beginning of the generator speeding up period to allow the maximum speed rising rate. As the speed goes up, the output power rises accordingly and settles to the steady-state value. On the contrary, during wind speed step down, the electrical torque is first increased, helping slow down the generator. The increase of electrical torque leads to higher generator output power, at the very beginning of the speed change. As the speed slows down, the active power decreases as well and settles to the steady-state value.

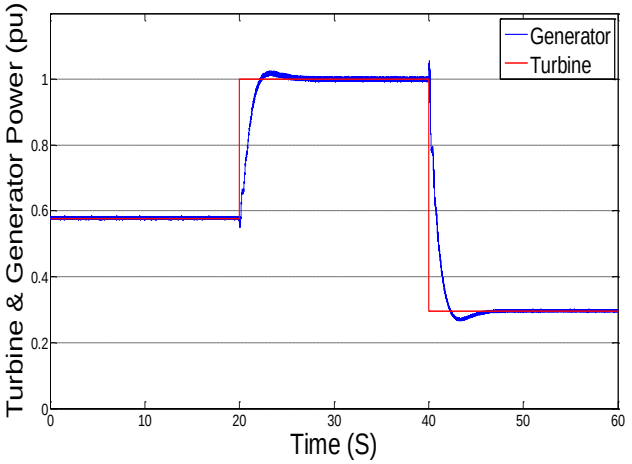

Fig. 11: Response of the generator and grid active power for BBO technique.

The reactive power responses of the grid for the BBO and GA optimization techniques are shown in Fig. 13 and Fig. 14, respectively. In Fig, 13 and 14, the reactive power is maintained at zero at the grid side for either steady state or transient operation, and unity power factor is kept regardless of the amount of real power.

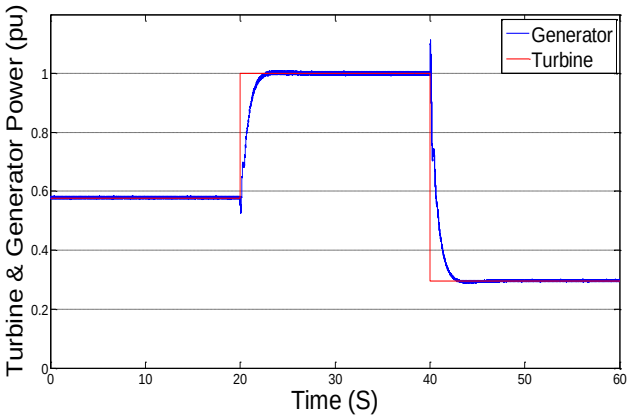

Fig. 12: Response of the generator and grid active power GA technique

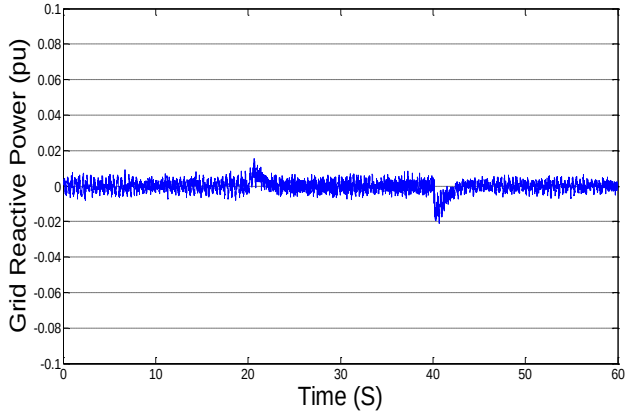

Fig. 13: Response of the grid reactive power for BBO technique

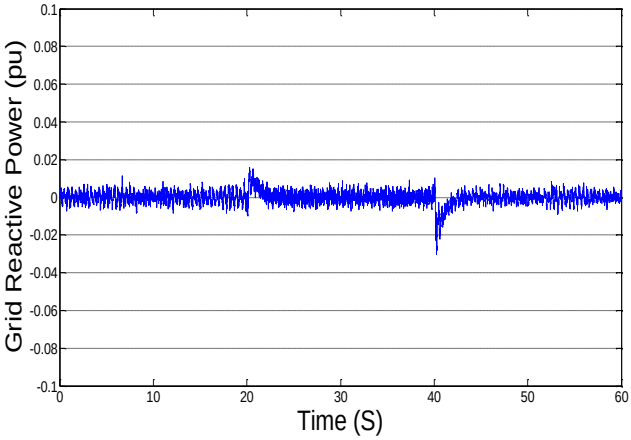

Fig. 14: Response of the grid reactive power for GA technique.

Fig. 15 and Fig. 16 show the response of the d-q current components of the PMSG with controller parameters optimized using BBO and GA, respectively. The d-axis current is zero during all the simulation time to get the maximum torque/ampere. The q-axis current is directly tracking the electromagnetic torque. Therefore, it is decreasing when the rotor speed has to increase in order to obtain a bigger acceleration. The current goes to the value which makes the electromagnetic torque equal to the wind turbine torque when the rotor speed reference is met.

Fig. 17 and Fig. 18 show the response of the d-q current components of the grid with controller parameters optimized using BBO and GA, respectively. The grid q-axis current is set all over the simulation to zero to get zero reactive power (unity power factor). The d-axis component is directly tracking DC link voltage.

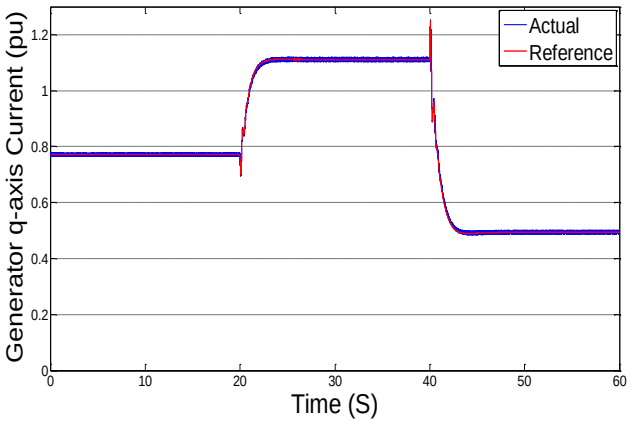

(a)

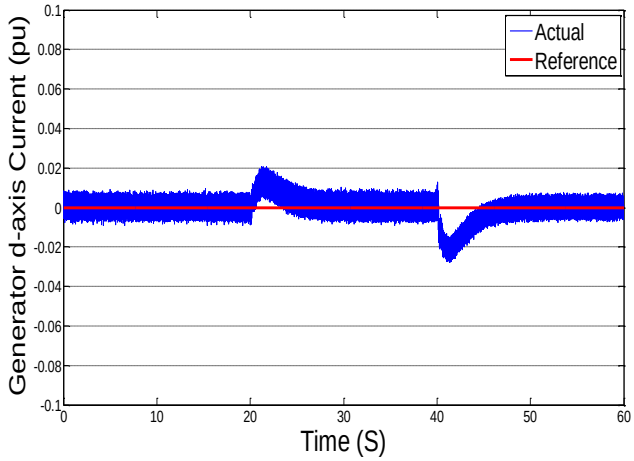

(b)

Fig. 15: Response of the d-q current components of the PMSG for BBO technique

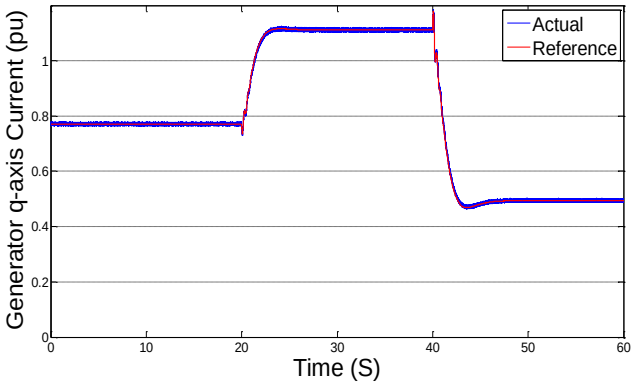

(a)

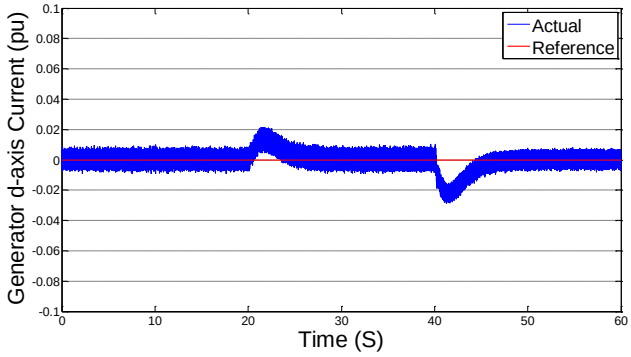

(b)

Fig. 16: Response of the d-q current components of the PMSG for GA technique

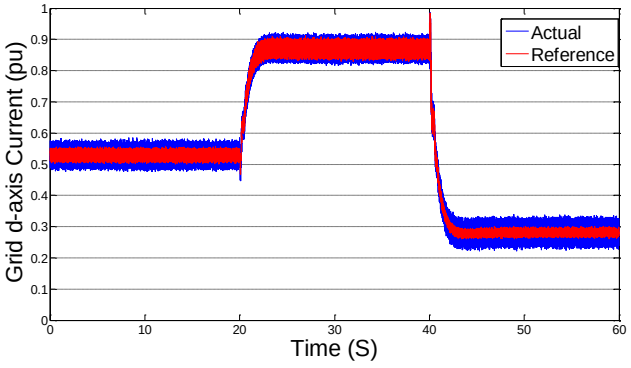

(a)

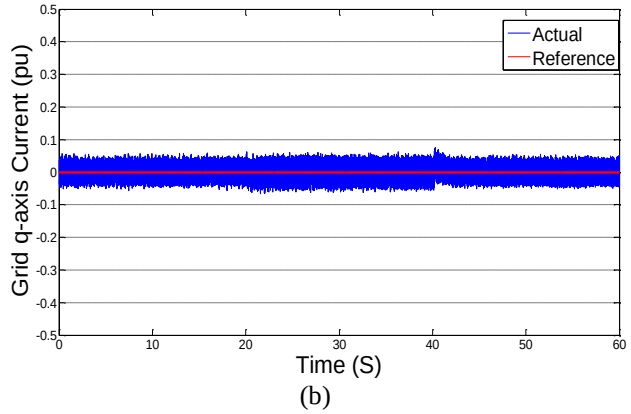

(b)

Fig. 17: Response of the d-q current components of the grid for BBO technique

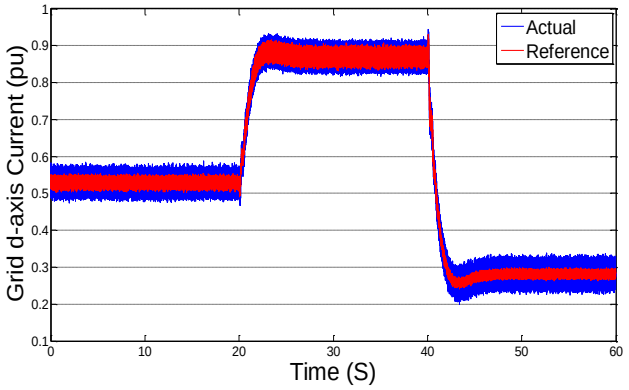

(a)

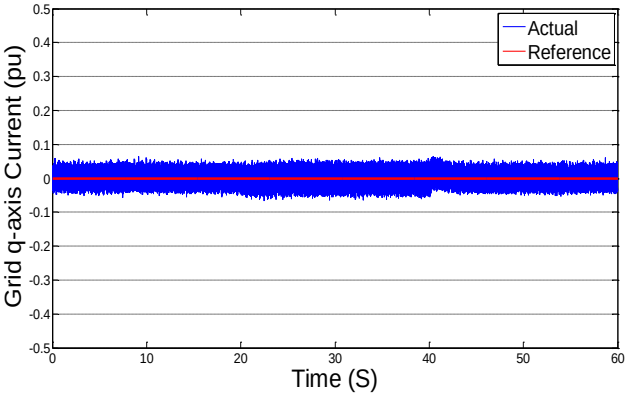

(b)

Fig. 18: Response of the d-q current components of the grid for GA technique

7. Conclusion

This paper has attempted to present an approach to optimally determine the controller parameters which control the frequency converter used in VSWT-PMSG to achieve MMPT. The Field oriented control is used to control the frequency converter using the PI controllers to obtain MPPT. Due to the nonlinearity of the wind generation system, the setting of the converters PI controller's parameters is difficult.

The maximum power point tracking, the difference between the reference and actual generator speed, and the difference between the reference and actual dc link voltage were considered as the objective functions. The minimization of the settling time, maximum overshoot and undershoot of the generator speed and the DC link voltage to track the reference values are considered as the performance indices to achieve MPPT.

The constrained optimization problem is solved using BBO. The effectiveness of the designed parameters using BBO is then compared with that obtained using genetic algorithm (GA).

The validity of the proposed methodology is confirmed through the simulation results. The effectiveness of the proposed methodology is verified for step change in wind speed. The overshoots, undershoots and settling time of DC link voltage response and generator speed response have reduced with optimal parameters obtained using BBO and the proposed BBO technique achieves the MPPT.

The detail of the optimum design procedure is discussed, which can be applied to other inverter/converter topology used widely in variable speed wind energy conversion systems.

Finally, it is concluded that BBO optimization technology might be a good choice for optimum design of controller parameters.

APPENDIX A
Wind Turbine Parameters

Parameter	Value
C1	0.5176
C2	116
C3	0.4
C4	5
C5	21
C6	0.0068
B	0°

APPENDIX B
Parameters of the PMSG-Based WECS

Parameters of the WECS in the simulations are converted to a pu system and the real values can be derived by multiplying each pu value and the base value. The system base values are defined as follows [27]:

$$I_b = \frac{P_b}{3V_b}, Z_b = \frac{V_b}{I_b}, \omega_b = 2\pi f_b, \omega_{bm} = \frac{\omega_b}{p}$$

$$L_b = \frac{Z_b}{\omega_b}, C_b = \frac{1}{\omega_b Z_b}, T_b = \frac{P_b}{\omega_{bm}}$$

$$J_b = \frac{2P_b p^2}{\omega_b^2}, K_b = \frac{2P_b p^2}{\omega_b}, \psi_{rb} = \frac{\sqrt{2}V_b}{\omega_b}$$

Where the variables with subscript "*b*" represent the base values; *P, V, I, f* are the power, voltage, current, and electrical frequency, respectively; *Z,L,C* are the impedance, inductance, and capacitance, respectively; ω, ω_m are the electrical and mechanical angular frequencies, respectively; *T* is the torque; *J,K* are the inertia and stiffness, respectively; *p* is the pole pairs of PMSG; and ψ_r is the amplitude of the flux induced by the permanent magnets of the rotor.

Base power *Pb* (MVA)	1.5
Base voltage *Vb* (V)	$690/\sqrt{3}$
Base frequency *fb* (Hz)	11.5
Pole pairs of PMSG *p*	40
Nominal WT mechanical power (pu)	1.1
Nominal WT speed (pu)	1.2
WT inertia constant (pu)	4.8
PMSG inertia constant (pu)	0.5
Shaft stiffness (pu)	2
Rated generator torque (pu)	1
Rated generator power (pu)	1
Rated generator line voltage	1
Rated generator speed (pu)	1
Generator inductance in the d frame (pu)	0.7
Generator inductance in the q frame (pu)	0.7
Generator stator resistance (pu)	0.01
Flux of the permanent magnets (pu)	0.9
DC-link capacitance (pu)	1
Line inductance (pu)	0.1
Rate wind speed (m/s)	12

References

1. Abdullah MA, Yatim AHM, Tan CW.: *A study of maximum power point tracking algorithms for wind energy system.* In: Proceedings of the 1st IEEE conference on clean energy and technology (CET), 2011, pp. 321–326.
2. Saidur R, Islam MR, Rahim NA, Solangi KH.: *A review on global wind energy policy*. In: Renewable and Sustainable Energy Reviews, vol. 14, 2010, pp. 1744–1762.
3. *Global Wind Report Annual Market Update 2013*. Global Wind Energy Council (GWEC) [Online]. Available: http://www.gwec.net.
4. Q. Wang and L. Chang: *An intelligent maximum power extraction algorithm for inverter-based variable speed wind turbine systems*. In: IEEE Transactions Power Electron., vol. 19, Sept. 2004, pp. 1242-1249.
5. Y. Zhao, C. Wei, Z. Zhang, and W. Qiao: *A review on position/speed sensorless control for permanent-magnet synchronous machine-based wind energy conversion systems.* In: IEEE J. Emerging and Selected Topics in Power Electron., vol. 1, no. 4, Dec. 2013, pp. 203-216.
6. Molina MG, dos Santos EC, Pacas M.: *Advanced power conditioning system for grid integration of*

direct-driven PMSG wind turbines. In: IEEE Energy Conversion Congress and Exposition (ECCE), 2010, pp. 3366–3373.

7. Li S, Haskew TA, Xu L.: *Conventional and novel control designs for direct driven PMSG wind turbines.* In: Electric Power Systems Research, vol. 80, 2010, pp. 328–338.
8. Muyeen SM, Takahashi R, Murata T, Tamura J.: *A variable speed wind turbine control strategy to meet wind farm grid code requirements.* In: IEEE Transactions on Power Systems, vol. 25, 2010, pp. 331–340.
9. G. Hua and Y. Geng.: *A novel control strategy of MPPT tracking dynamics of wind turbine into account.* In: Proc. IEEE Power Electron. Spec. Conf., Jun. 2006, pp. 1-6.
10. K.-H. Kim, D.-C. Lee, and J.-M. Kim.: *Fast tracking control for maximum output power in wind turbine systems.* In: Proceedings of AUPEC, December 2010, pp. 1-5.
11. H. Polinder, S.W. H. de Haan, M. R. Dubois, and J. Slootweg.: *Basic operation principles and electrical conversion systems of wind turbines*. In: Proceedings of the Nordic Workshop Power Ind. Electron. , June 2004, pp. 14–16, Norway.
12. G. Michalke, A. D. Hansen, and T. Hartkopf.: *Control strategy of a variable speed wind turbine with multipole permanent magnet synchronous generator*. In: Proceedings of the Eur.Wind Energy Conf. Exhib. , May 2007, pp. 7–10, Milan, Italy.
13. Hasanien H. M, Muyeen S. M.: *Design Optimization of Controller Parameters used in Variable Speed Wind Energy Conversion System by Genetic Algorithms*. In: IEEE Transactions on Sustainable Energy, vol.3, April 2012, pp.200- 208.
14. A. Ghaffari, M. Krstić, and S. Seshagiri.: *Power optimization and control in wind energy conversion systems using extremum seeking.* In: Proceedings of the American Control Conference (ACC), 2013, pp. 2241-2246.
15. D. Simon. *Biogeography-based optimization.* In: IEEE Transactions on Evolutionary Computation, vol. 12, December 2008, pp. 702-713.
16. Y. Xia, K. H. Ahmed, and B. W. Williams: *Wind turbine power coefficient analysis of a new maximum power point tracking technique*. In: IEEE Transactions on Industrial Electronics, vol. 60, March 2013, pp. 1122-1132.
17. Siegfried Heier.: *Grid Integration of Wind Energy Conversion Systems*. John Wiley & Sons Ltd, ISBN 0-471-97143-X, 1998.
18. T. H. Nguyen, S.-H. Jang, H.-G. Park, and D.-C. Lee.: *Sensorless control of PM synchronous generators for micro wind turbines.* In: Proceedings of IEEE 2nd Int. Power Energy Conf., December 2008, pp. 936–941.
19. J. Dai, D. Xu, B.Wu, and N. R. Zargari.: *Unified DC-link current control for low-voltage ride-through in current-source-converter-based wind energy conversion systems*. In: IEEE Trans. Power Electron., vol. 26, Jan. 2011, pp. 288–297.
20. G. Foo and M. F. Rahman.: *Sensorless direct torque and flux-controlled IPM synchronous motor drive at very low speed without signal injection*. In: IEEE Transactions Power Electron., vol. 57, Jan. 2010, pp. 395–403.
21. Busca, C., et al., et al.: *Vector control of PMSG for wind turbine applications*. In: s.l.: Dept. of Energy Technol., Aalborg Univ., Industrial Electronics (ISIE), Aalborg, Denmark, 2010, pp. 3871 - 3876.
22. YANG Yong, RUAN Yi, SHEN Huan-qing, and TANG Yan-yan.: *Grid-connected inverter for wind power generation system*. In: J Shanghai Univ, 2009, pp. 51–56.
23. A. Wallace.: *The Geographical Distribution of Animals*. (Two Volumes). Boston, MA: Adamant Media Corporation, 2005.
24. C. Darwin.: *The Origin of Species*. New York: Gramercy, 1995.
25. T. Wesche, G. Goertler, and W. Hubert.: *Modified habitat suitability index model for brown trout in southeastern Wyoming*. In: North Amer. J. Fisheries Manage., vol. 7, 1987, pp. 232–237.
26. T. Back.: *Evolutionary Algorithms in Theory and Practice*. In: Oxford University Press, 1996.
27. Geng, H.; Yang, G.; Xu, D.; Wu, B.: *Unified power control for PMSG-based WECS operating under different grid conditions.* In: IEEE Transactions Energy Convers., vol. 26, 2011, pp. 822–830.